

Draft August 5, 2018

The Mass Distribution of Stellar Black Holes

Charles D. Bailyn¹

Yale University, Department of Astronomy, P.O. Box 208101, New Haven, CT 06510-8101
E-mail: bailyn@astro.yale.edu

Raj K. Jain & Paolo Coppi

Yale University, Department of Physics, P.O. Box 208101, New Haven, CT 06510-8101
E-mail: raj.jain@yale.edu, coppi@astro.yale.edu

Jerome A. Orosz

Pennsylvania St. University, Dept. of Astronomy & Astrophysics, 525 Davey Lab,
University Park, PA 16802-6305
E-mail: orosz@astro.psu.edu

ABSTRACT

We examine the distribution of masses of black holes in transient low mass X-ray binary systems. A Bayesian analysis suggests that it is probable that six of the seven systems with measured mass functions have black hole masses clustered near seven solar masses. There appears to be a significant gap between the masses of these systems and those of the observed neutron stars. The remaining source, V404 Cyg, has a mass significantly larger than the others, and our analysis suggests that it is probably drawn from a different distribution. Selection effects do not appear to play a role in producing the observed mass distribution, which may be explained by currently unknown details of the supernova explosions and of binary evolution prior to the supernova.

Subject headings: binaries: spectroscopic — black hole physics — supernovae — X-rays: binary

¹National Young Investigator

1. Introduction

The strongest case for the existence of black holes in nature is provided by a subclass of X-ray transients. The strong episodic X-ray emission from these binary stars demonstrates the existence of an accreting compact object. Radial velocity measurements of the companion star can be used to determine the mass function, which is a strict lower limit to the mass of the compact accretor. In a number of cases, this lower limit is above the upper limit of neutron star stability of $3M_{\odot}$ (McClintock & Remillard 1986, Casares & Charles 1992, Remillard, McClintock & Bailyn 1992, Bailyn et al. 1995, Filippenko et al. 1995, Remillard et al. 1996). In these cases the compact object must be a black hole.

Studies of the supernovae explosions which presumably give rise to these black holes have now progressed to the point where meaningful statements can begin to be made about the expected mass distribution of the black holes. Studies of galactic chemical evolution strongly imply that stars with initial masses above $\approx 30M_{\odot}$ must “swallow” many of their heavy elements during (or shortly after) the supernova event, and therefore should form relatively massive black holes (Maeder 1992, Timmes, Woosley & Weaver 1995). Detailed models of the supernovae explosions themselves (e.g. Timmes, Woosley & Weaver 1996) can reproduce this result by applying a fixed amount of kinetic energy to the outer layers of the star, and determining how much material recollapses onto the central object. However, there remain many uncertainties in the relation between the initial mass of the star and the mass of the compact remnant left behind by the supernova. The amount of kinetic energy available, how it is transferred to the ejected material, details of the pre-supernova evolution of massive stars (especially relating to convection and mass loss) and the possible influence of a binary companion are all poorly understood. In this paper, therefore, we take an empirical approach — we attempt to use the available observational evidence for stellar black holes with low mass companions (high mass systems such as Cygnus X-1 presumably having followed a different evolutionary path), and see what constraints can be made upon the underlying distribution of black hole masses.

The mass of the black hole primary m_1 is related to the observed mass function $f(m)$ in the following way:

$$m_1 = \frac{f(m)(1+q)^2}{\sin^3 i} \quad (1)$$

In order to determine the mass of the black hole, one needs to know the mass ratio q and the inclination i of the binary system. These parameters can be measured, although somewhat more indirectly than the mass function, as discussed in section 2 below. Section 2 also presents a compilation of the data obtained on those low mass X-ray transients with measured mass functions which do not display X-ray bursts (generally considered to be a

neutron star signature). In section 3, we use these data to examine the distribution of black hole masses following the Bayesian analysis employed by Finn (1994) in his study of neutron star masses. Our results suggest that V404 Cyg is not drawn from the same population as the other six sources, and that the group of six have black hole masses which cluster around $7M_{\odot}$ with a significant gap between their distribution and that of the neutron stars. In section 4 we speculate about the implications of our results.

2. Constraints on Black Hole Masses

As can be seen in Equation 1, the mass ratio and inclination of the binary system are required in addition to the mass function to determine the mass of the black hole primary. These quantities have been measured in a variety of ways, which are discussed in sections 2.1 and 2.2. Section 2.3 evaluates the currently available data on each of the seven systems being considered.

2.1. Determining the Mass Ratio

The most conceptually straightforward way to determine the mass ratio of a binary system is by measuring a velocity curve for both components of the binary system. Therefore several attempts have been made to construct an orbital velocity curve for the emission lines emanating from the accretion disks in black hole binaries (e.g. Orosz et al. 1994). Such a velocity curve should track the motion of the primary; the ratio of its amplitude to that of the velocity curve of the absorption spectrum of the secondary determines the mass ratio. However, the emission line velocity curve is observed to lag behind its expected phase, and thus cannot reflect the true motion of the primary (Orosz et al. 1994). Thus this method, while conceptually simple, is suspect in practice. Curiously, despite the phase lag, the results obtained by naively applying this method agree with those of other methods.

A more reliable method for determining the mass ratio is to observe the rotational broadening of the lines from the secondary star. The secondary fills its Roche lobe, and the ratio of its effective radius to the orbital semi-major axis is therefore determined by the mass ratio. By comparing the projected orbital velocity of the secondary (as determined by the velocity curve) and the projected rotational velocity observed from the line broadening, the mass ratio can be determined. This procedure is thought to be reliable, but the observations require relatively high dispersion and signal to noise, and are thus not feasible

for the faintest systems.

The secondaries of these system are generally undermassive for their spectral types when compared to typical main sequence stars. Presumably this is because they are not in thermal equilibrium, due to the ongoing mass loss. In cases where the rotational broadening cannot be observed, crude limits on the mass of the secondary can be set by assuming that the secondary is somewhat less massive than a main sequence star of similar spectral type.

2.2. Determining the Inclination

The orbital inclination can in principle be determined by observing the ellipsoidal variability of the Roche lobe filling secondary. This has been done with high precision in the case of GRO J1655-40 (Orosz & Bailyn 1997). In this case, the shapes of the lightcurves were sufficiently accurately determined that the mass ratio could also be determined from the models. However in other cases, the lightcurves are modified by several effects, which can only be modelled approximately.

There is a contribution of light from the disk, which is approximately constant throughout the orbit, and thus decreases the ellipsoidal amplitude for a given inclination. The disk fraction can be determined by comparing the depths of the absorption features (produced by the secondary) with those of single stars, but the disk can vary from observation to observation, and also as a function of phase, so the correct disk fraction to apply is not in general well-determined. Another source of distortion for the lightcurves may be star spots on the rapidly rotating secondaries, which may be particularly important for late spectral types.

It is often assumed that light curves in the IR will be free of disk contamination, so ellipsoidal modelling of IR lightcurves is a favored method of determining the inclination. However it should be noted that in GRO J1655-40, the disk is actually redder than the secondary star in quiescence, so the assumption that the IR is relatively free of disk contamination may not be reliable.

2.3. Specific Systems

Here we briefly describe the data available on each of the seven systems. The results are summarized in Table 1, and in Figure 1, which shows the mass limits derived by considering the extremes of the errors and ranges listed in Table 1. The systems are listed in order of decreasing mass function.

GS 2023+34 = Nova Cyg 1938/1989 = V404 Cyg: This source has the highest measured mass function of any compact object (Casares & Charles 1994) and is therefore the strongest case for a black hole. Casares & Charles (1994) also derive the mass ratio from rotational broadening, and Pavlenko et al. (1996) confirm the inclination limits found by Shahbaz et al. (1994) from ellipsoidal modelling of the IR light curve.

GS 2000+25 = Nova Vul 1988: The best values for the mass function and the mass ratio from rotational broadening were reported by Harlaftis et al. (1996). The limits on the inclination are derived from ellipsoidal modelling of the IR light curve by Beekman et al. (1996).

H 1705-25 = Nova Oph 1977: The best value for the mass function of this system is given by Filippenko et al. (1997). The mass ratio is adopted to fit the limits on rotational broadening given by Harlaftis et al. (1997). The range of inclinations is from ellipsoidal modelling of the optical light curve by Remillard et al. (1996).

GRO J1655-40 = Nova Sco 1994: This source displays remarkably precise ellipsoidal variations in quiescence, which have allowed us to determine the mass ratio and inclination of the system to unprecedented precision (Orosz & Bailyn 1997). The excellent fits are presumably due to the relatively early spectral type of the secondary (F5) which decreases the effects of starspots, and the very small contribution from the disk ($\leq 5\%$). This is the only case among these sources in which the shape of the ellipsoidal lightcurve is sufficiently well-determined to provide a strong constraint on the mass ratio. The formal error on the inclination quoted by Orosz & Bailyn is only $\pm 0.1^\circ$, but we use a larger range here which encompasses several other local minima in χ^2 , even though these minima are formally several sigma less significant than the overall best fit at $i = 69.50^\circ \pm 0.08$.

GS 1124-68 = Nova Mus 1991: The most recent results for the mass function and inclination of this source are given by Orosz et al. (1996). The mass ratio is determined from the observed rotational velocity by Casares et al. (1997) and agrees with the results from the emission line velocity curve given by Orosz et al. (1994).

A 0620-00 = Nova Mon 1975 = V616 Mon: This source was the first of its class for which a mass function was determined (McClintock & Remillard 1986). The source has been extensively studied over the past decade by many authors. However there remain sharp disagreements over the inclination. Ellipsoidal variability measurements in the IR give inclinations in the range of $31^\circ \leq i \leq 54^\circ$ (Shahbaz et al. 1994a), while lightcurves in the optical and rotational velocity measurements yield much higher inclinations (e.g. Haswell et al. 1993). Rather than attempt to resolve this discrepancy here, we simply adopt the entire range of reported results. This large range of inclinations yields a correspondingly

large range in values for the primary mass. In contrast, all of the various measurements of the mass ratio yield consistent results.

GRO J0422+32 = Nova Per 1992: This is the only source included here with a mass function significantly less than $3M_{\odot}$ (Filippenko et al. 1995). However it displayed no X-ray bursts, and there are a number of indications that the inclination is relatively low, and that therefore the primary mass is in the black hole range. However, attempts to determine the inclination by studying ellipsoidal variations have been ambiguous, probably because the effects of starspots are particularly acute for this relatively late type secondary (M0). Orosz & Bailyn (1995) report an inclination of $\approx 45^{\circ}$, but this conclusion was undermined by subsequent data which revealed a smaller ellipsoidal amplitude when the source was 0.2 magnitudes fainter, which goes in the wrong direction for a change in disk contamination (Callanan et al. 1996). The results of Callanan et al. (1996) clearly indicate that $i < 45^{\circ}$; as a lower limit, we adopt an inclination which provides just enough ellipsoidal variability to produce the smallest observed ellipsoidal modulation in the complete absence of disk contamination.

3. Application of Bayesian Statistics

Figure 1 shows the ranges over which the primary masses of the seven sources can vary, given the observational constraints. It is important to note that these mass limits cannot be interpreted as coming from gaussian distributions that are characterized by some “sigma.” The heterogeneous nature of the observed quantities, and the non-linear ways they enter into the calculation of the primary mass, mean that the probability for a black hole to be at a given point between the plotted limits varies in a strongly non-gaussian manner. Therefore, to learn more about the black hole masses and, in particular, to see what parent mass distribution they could have been drawn from, we have performed a Bayesian analysis similar to that used by Finn (1994) to study the distribution of neutron star masses in binary systems.

Bayesian analysis is a powerful tool that allows one to quantify the consistency of a particular model, in this case a parent distribution of black hole masses, with a set of data taking into account any “prior” knowledge (biases) we might have concerning the systems being studied along with the observational uncertainties involved in obtaining the data. In brief (e.g., see Loredo 1990), the Bayesian approach does not assign error bars to data but rather starts with a model that is supposed to describe the system that produced the data. It then asks what is the likelihood for that particular model to be relevant or correct in the first place (based on any prior knowledge or biases we may already have concerning the

system), and finally it asks what is the likelihood the data points could have been generated by the model given what we understand about the measurement process that produced the data points. To those new to Bayesian analysis, this approach often seems backwards and troubling since one usually thinks of the data as the starting point for any analysis and also feels strongly that the final answer should be objective, i.e., not depend on the prior knowledge of the observer. However, the process of Bayesian inference actually matches closely the process of how the scientific community arrives at what it considers to be scientific knowledge (e.g., an apparently significant experimental result is ignored because everyone knows the detector “is always broken”) and is “honest” in the sense that all the underlying assumptions are spelled out explicitly. Also, Bayesian analysis is not quite as subjective as it might first appear. For many classes of problems, one can show that there exists a unique set of prior knowledge or assumptions that is “reasonable” in the sense that it is “minimally biased” or contains the “least amount” of prior information. Although the approach of starting with a well-specified model instead of the data can be computationally cumbersome, it makes maximum use of the available information and often allows one to make significant, quantitative statements about model-data consistency even when the data are sparse, as is the case here. But it should be remembered that conclusions based on a Bayesian analysis always depend critically on the assumed models and prior knowledge (biases).

3.1. Method

To start our Bayesian analysis, we must put down the assumptions and models for our particular problem. Since we have only seven black hole systems for study, we do not expect to be able to make very detailed statements about any particular parent distribution for black hole masses. Accordingly, we shall only consider a very simple model where the masses of the black hole primaries are uniformly distributed between between some lower and upper mass limits, m_l and m_u respectively. Our set of prior knowledge, which we denote \mathcal{I} , includes the available information (discussed above) for the inclinations and mass ratios of individual systems, the assumption that our model mass distribution is correct, broad bounds on the possible values of m_l and m_u , and the assumption that all values of m_l and m_u are *a priori* equally probable within those bounds, provided $m_l \leq m_u$. Given this prior knowledge, our goal is then to determine the probability density function $P(m_l, m_u | f_n, \mathcal{I})$, which tells us how likely it is for the mass distribution specified by a particular choice of m_l and m_u to be the correct one given the set of observed mass functions f_n (our data). We will express our results in terms of probability contours in the (m_l, m_u) plane.

Bayes' Theorem, applied to this problem, states that

$$P(m_l, m_u | \{f_n\}, \mathcal{I}) = \frac{P(m_l, m_u | \mathcal{I}) P(\{f_n\} | m_l, m_u, \mathcal{I})}{P(\{f_n\} | \mathcal{I})}. \quad (2)$$

The quantities on the right hand side of equation 2 are interpreted in the following manner. The first term of the numerator $P(m_l, m_u | \mathcal{I})$ is the probability that a given combination of m_l and m_u is allowed by our prior information. We will take this probability to be uniform for $m_l \leq m_u$ and $0.5M_\odot \leq m_l, m_u \leq 30M_\odot$, and zero otherwise. This mass range was chosen to encompass the entire reasonable range of black hole masses in transient systems. Since P must integrate to unity over all m_l and m_u , we find that

$$P(m_l, m_u | \mathcal{I}) = \frac{2}{(30 - 0.5)^2} \quad (3)$$

within the bounds given above, where we have chosen to measure the (m_l, m_u) plane in units of solar masses.

The second term in the numerator, $P(\{f_n\} | m_l, m_u, \mathcal{I})$, is the probability of obtaining a specific set of observations $\{f_n\}$ given our prior assumptions, and specific values of m_l and m_u . Since the observations of the individual black holes are independent of each other we can factorize $P(\{f_n\} | m_l, m_u, \mathcal{I})$ as follows:

$$P(\{f_n\} | m_l, m_u, \mathcal{I}) = \prod_i P(f_i | m_l, m_u, \mathcal{I}) \quad (4)$$

where $f_{i=1,n}$ are the mass functions obtained for the individual sources. The product rule of probability yields

$$P(f_i | m_l, m_u, \mathcal{I}) = \int d\hat{f}_i P(f_i | \hat{f}_i, \mathcal{I}) P(\hat{f}_i | m_l, m_u, \mathcal{I}) \quad (5)$$

where \hat{f}_i is the true value of the mass function, and f_i is the observed value. We will assume that the relationship between the true and observed values of the mass function is given by a gaussian probability distribution with σ equal to the error in f_i quoted by the observers. Thus

$$P(f_i | \hat{f}_i, \mathcal{I}) = \exp[-\frac{1}{2}(\frac{f_i - \hat{f}_i}{\sigma})^2] / 2\pi\sigma. \quad (6)$$

The function $P(\hat{f}_i | m_l, m_u, \mathcal{I})$ is the likelihood for the true value of the mass function to be \hat{f}_i given \mathcal{I} and particular values of m_l and m_u . Since the black hole mass

$$m_i = \hat{f}_i(1 + q)^2 / \sin^3 i, \quad (7)$$

we can change variables and write

$$P(\hat{f}_i|m_l, m_u, \mathcal{I}) = \int \int didq P(m_i)P(i)P(q) \frac{(1+q)^2}{\sin^3 i} \quad (8)$$

where $P(m_i)$ is uniform for $m_l \leq m_i \leq m_u$ and zero otherwise, $P(q)$ is a gaussian given by the mean value and error quoted in Table 1, and $P(i) \propto \sin i$ (i.e. $P(\cos i)$ is uniform) between the bounds given in Table 1 and zero elsewhere, normalized to yield unity when integrated over all angles. If we compute m_i for each value of q and i using equation 7, the integral in equation 8 can be computed using standard methods for any given value of \hat{f}_i , and these results can be used to compute $P(\{f_n\}|m_l, m_u, \mathcal{I})$ using equations 6 and 4.

Finally, the remaining term in the right hand side of equation 2, $P(\{f_n\}|\mathcal{I})$, is the “prior predictive probability” or “global likelihood” of the model under consideration. This term represents the probability that the observed set of $\{f_n\}$ can be obtained given our set of prior knowledge and assumptions, \mathcal{I} . For our problem, this represents the probability that the black hole mass distribution for our seven systems can be correctly modeled as a uniform distribution between two mass limits, m_l and m_u , constrained to lie between $0.5M_\odot$ and $30M_\odot$. In most Bayesian analyses, this term is to be regarded as a normalization constant. The left hand side of equation 1 must by definition have a value of unity when it is integrated over all possible values of m_l and m_u , and this requirement fixes $P(\{f_n\}|\mathcal{I})$ if the other quantities on the right-hand side of equation 2 are known, ie.,

$$P(\{f_n\}|\mathcal{I}) = \int_{0.5}^{30} \int_{0.5}^{30} dm_u dm_l P(\{f_n\}|m_l, m_u, \mathcal{I}) P(m_l, m_u|\mathcal{I}). \quad (9)$$

The global likelihood of a model is a very useful quantity as it allows one to objectively compare classes of models. Larger values of the global likelihood imply that the underlying model is more likely to be correct. Specifically, the ratio of the global likelihood of two models can be shown to constitute an “odds ratio” which compares one model to the other (Loredo 1990). To see this result, let us assume that we add an extra piece of information, \mathcal{I}' to our prior knowledge. This new information states that we assume that our data could be explained by some number N of possible models and that only one of these models, we don’t know which, is actually the right one. Then using Bayes theorem, we can write

$$P(M_i|\{f_n\}, \mathcal{I}, \mathcal{I}') = P(M_i|\mathcal{I}, \mathcal{I}') \frac{P(\{f_n\}|M_i, \mathcal{I}, \mathcal{I}')}{P(\{f_n\}|\mathcal{I}, \mathcal{I}')} \quad (10)$$

where M_i refers to the i^{th} of the models we are considering and $P(M_i|\mathcal{I}, \mathcal{I}')$ is our prior probability for that model to be correct. The expression $P(\{f_n\}|M_i, \mathcal{I}, \mathcal{I}')$ is the probability that we reproduce the data given (i) our prior set of knowledge \mathcal{I} ; (ii) that a set of possible models \mathcal{I}' exists; and (iii) that of these models, M_i is the correct one. Since we assumed

that only one model could be correct, clearly this probability is independent of the existence of any alternative models, $M_{i \neq j}$. Hence, this probability is the same as $P(\{f_n\}|M_i, \mathcal{I})$, the probability that we can reproduce our data using model M_i constrained by our original set of prior knowledge, i.e., it is the global likelihood for model M_i (calculated in the manner described above by integrating over all the possible parameters of the model). Knowing this we can now calculate the odd's ratio, O_{ij} , favoring one of the models, M_i , over another, M_j ,

$$O_{ij} = \frac{P(M_i|\mathcal{I}') P(\{f_n\}|M_i, I)}{P(M_j|\mathcal{I}') P(\{f_n\}|M_j, I)}. \quad (11)$$

In other words, the probability favoring a model as a whole is proportional to its prior probability times its global likelihood. In what follows, we shall assume that we have no prior knowledge of which M_i is correct and set all the $P(M_i|\mathcal{I}')$ equal. Thus the odds favoring one model over another is simply the ratio of the global likelihoods.

Our overall procedure used to compute all the required probabilities is as follows. We take a grid of values of m_l and m_u in the range $0.5M_\odot \leq m_l \leq m_u \leq 30M_\odot$. For each pair of (m_l, m_u) values, we compute $P(f_i|m_l, m_u, \mathcal{I})$ for each source by integration as described above. The results for each source are then multiplied together to get $P(\{f_n\}|m_l, m_u, \mathcal{I})$ for each grid point in (m_l, m_u) space. We next sum these values over m_l and m_u , and determine a value for the global likelihood $P(\{f_n\}|\mathcal{I})$ such that the sum of $P(m_l, m_u|\{f_n\}, \mathcal{I})$ is unity, as required.

3.2. Results

The results of applying this method to the full data set of seven objects is shown in Figure 2. The contour enclosing 95% of the probability covers a region with $11 \leq m_u/M_\odot \leq 17$, and $m_l/M_\odot \leq 7$. The maximum likelihood point is at $m_l = 5.5M_\odot$ and $m_u = 11.7M_\odot$.

A more intriguing result is obtained by modifying one of the assumptions implicit in \mathcal{I} . Instead of assuming all the black hole masses are drawn from the same parent mass distribution, we assume that the masses of only six of the objects are drawn from this distribution and that the mass of the seventh comes from a different one. For simplicity, we will assume that the mass of the seventh is in fact known to have some value consistent with the data so that the probability $P(f_7|\mathcal{I})$ equals unity and that object effectively drops out of the computation. Assuming that each system in turn has a known mass, we compute a corresponding global likelihood for the resulting model. (This is the same likelihood as before except we now consider only the six remaining objects). The surprising set of

likelihood values we obtained is shown in Table 2. By comparing these global likelihood values to each other and to the one we obtained above, we can ascertain whether a particular model is “favored” relative to the others. In most cases, removing one object made little difference to the either the global likelihood or the shape of the contours for the model probability distribution (as a function of m_l and m_u). However, when GS 2023+34 (V404 Cyg) was removed, the change was dramatic (see Figure 2).

When sources other than V404 Cyg were left out, the model global likelihoods rose by only factors of a few. (They rose presumably because our assumption that m_u could be as high as $30M_\odot$ was wrong — with each additional source this assumption becomes less plausible). By contrast, when V404 Cyg was removed, the global likelihood of the model rose by over two orders of magnitude. This strongly suggests that V404 Cyg is indeed drawn from a different distribution than the other sources. It should be noted that V404 Cyg is also unusual in having a longer orbit and more evolved secondary than the other sources.

Looking at the probability contours when V404 Cyg is left out, the maximum likelihood values of m_l and m_u become much closer ($m_l = 6.91$ and $m_u = 6.97$). Indeed, there is considerable probability that $m_l = m_u$, i.e. that the distribution can be plausibly modelled by a single black hole mass near $7M_\odot$. Figure 3 shows the probability that m_l and m_u are within some value of each other. This plot was generated by integrating over the normalized probability distribution for all $m_u - m_l \leq \Delta m$. When all seven sources are considered, the distribution cannot be narrower than $4M_\odot$ wide (i.e. $\Delta m \geq 4M_\odot$). When V404 Cyg is not included, over 50% of the probability has $\Delta m \leq 2M_\odot$. This result suggests that the possibility that many black holes have masses in a small range near $7M_\odot$ should be seriously considered.

Another effect of leaving out V404 Cyg is that the likely values for m_l becomes much higher. Figure 5 shows the probability that m_l is below some value. As can be seen, there is a 95% probability that $m_l > 3M_\odot$, and a 90% probability that $m_l > 4M_\odot$. Given the upper limit of $\leq 1.7M_\odot$ for the observed neutron star distribution, this result implies a considerable gap in the observed mass distribution of compact objects.

4. Discussion

The mass distribution of stellar mass black holes can in principle be predicted by models of the evolution and supernova explosions of massive stars. Timmes et al. (1996 — hereafter TWW) for example find that compact remnants of supernovae become significantly more massive than the pre-supernova iron core when the progenitor’s initial

mass exceeds $30M_{\odot}$. Above this mass, the kinetic energy of the explosion is insufficient to unbind the entire mantle and envelope of the star, so some of the outer regions fall back hole the core, increasing the mass of the remnant. Studies of galactic chemistry confirm that stars above $30M_{\odot}$ cannot return their entire outer regions to the interstellar medium (Maeder 1992, Timmes et al. 1995). Taking the reasonable assumption that the applied kinetic energy is only weakly dependent on the progenitor’s initial mass, TWW find a smooth monotonic relation between remnant and progenitor mass (see their Figure 1). If the initial mass function is weighted toward lower mass stars, as is almost certainly the case, the resulting mass distribution of black holes should be smooth, and strongly biased toward masses near those of the neutron stars.

While a sample including only seven examples cannot provide unambiguous statistical results, our work strongly suggests that the expected distribution is not observed. As discussed above, it is likely that one of the seven sources is not drawn from the same distribution as the other six. These six black holes may well be tightly clustered in mass near $7M_{\odot}$, although broader distributions are also possible. Finally, there is a significant gap between the lower mass limit of this distribution and the upper limit of the observed neutron star masses given by Finn (1994). The expected pile-up of sources at masses near to that of the neutron stars appears to be ruled out. Thus, although the small number of sources prevents us from drawing completely compelling conclusions, the evidence against the kinds of distributions implied by the work of TWW is strong enough to warrant serious consideration of the ways in which those distributions could be significantly modified.

A possible caveat is that this last conclusion might arise from observational selection effects. At present, however, we cannot think of any that would prevent systems with black hole masses near the neutron star upper limit from being detected. These sources are easy to identify — in outburst they are among the brightest objects in the X-ray sky. Also, the clear observation of similar systems containing accreting neutron stars strongly suggests that the mass of the compact object is not critical in the identification of these sources. Note that we have included *all* transient systems with measured mass functions in our sample, except those like Cen X-4 (McClintock & Remillard 1990) which display type I X-ray bursts, which are convincing signatures of the presence of a neutron star. In particular, we included GRO J0422+32, which is often left off lists of confirmed black holes because its mass function is well below the limit of $3M_{\odot}$ generally taken to be the firm upper limit for neutron star stability. It is conceivable that some effect suppresses the disk instability cycle over some mass range of the primary star, thus preventing the transient behavior needed to both identify the source in the first place, and then subsequently measure the mass function. Once again, however, the existence of transient sources with neutron star primaries and recurrence timescales similar to or smaller than those of the

black hole systems makes this solution implausible.

The physical effects which might influence the black hole distribution can be divided into two classes: those which involve the supernova explosion itself, and those related to the binary nature of the observed systems. Regarding the supernova explosions, if the relation between the amount of fall-back material to the mass of the precursor were close to a step function, then one might imagine that if *any* significant amount of material were to fall back, there would be enough to bring the total remnant mass up to $\approx 7M_{\odot}$. In this case, even if the amount of fallback material increased with increasing precursor mass after the initial step, one would still expect a strongly peaked distribution due to the steep expected mass function of massive stars. One conceivable scenario which might lead to such a step function is if some chemical transition within the precursor immediately prior to the supernova occurred just exterior to $\approx 7M_{\odot}$. Then the higher density and atomic number interior to the transition might result in precisely that portion of the star recollapsing, while the outer regions are expelled. Unfortunately, evolutionary calculations of very massive stars are subject to a number of important uncertainties (Woosley & Weaver 1995) particularly relating to mass loss rates, so this suggestion is hard to evaluate.

It may be that the observed distribution of black hole masses is not a result of type II supernova explosions in general, but rather a consequence of the binary nature of the observed systems. All of the orbital periods are sufficiently small that considerable mass transfer must have occurred prior to the supernova explosion. Since the precursor of the supernova was almost certainly more massive than its companion, it would have filled its Roche lobe first, resulting in dynamically unstable mass transfer. This in turn would result in a common envelope configuration, leading to the expulsion of much of the outer envelope of the more massive star and a dramatic decrease in the orbital separation on a very short timescale. Such abrupt mass loss has been shown to dramatically change the nature of the subsequent supernova explosion (Brown, Weingartner & Wijers 1996). However it is not clear how this set of circumstances could lead to a narrow range of remnant masses, or to a gap, since the effects of common envelope evolution are strongly dependent on the initial binary separation, which presumably is broadly distributed.

The mass of the black hole may also be influenced by mass accretion subsequent to the supernova event. If this effect changed the mass of the primary significantly, one would expect to see broadly distributed masses for the black hole, since the system should have undergone varying amounts of accretion after the formation of the compact object. Such a broadened distribution cannot currently be ruled out, but confirmation of the suggested sharp mass distribution would argue strongly against significant post-SN mass enhancement. In most cases there are also evolutionary arguments against post-SN mass enhancement.

Five of the seven systems in our sample contain late-type main sequence secondaries. These stars have masses $< 1M_{\odot}$, and it would require considerable fine tuning if they had all begun with much more massive secondaries. GRO J1655-40 has a secondary in the Hertzsprung gap — considerable ingenuity is required to reconcile this with the required low mass transfer rate for transient behavior (Kolb et al. 1997), and it is not clear how much mass transfer might have already taken place. The remaining system is V404 Cyg, whose secondary is at the base of the giant branch. In this case, considerable material may indeed have been transferred, which might conceivably account for the anomalously high mass of this particular black hole.

Thus, while there are a number of poorly understood effects which might alter the distribution of post-supernova remnant masses, it is not immediately obvious how these effects could combine to produce the kind of distribution favored by our analysis. Obviously, more examples of black hole systems and better measurements of known systems will result in more precise observational constraints using techniques such as the ones outlined here. But already it appears likely that we will have to consider new underlying mechanisms for the origin of the Galactic black hole mass distribution.

We are grateful for conversations with Richard Larson. CDB and RKJ acknowledge support from the National Science Foundation (National Young Investigators program).

REFERENCES

- Bailyn, C. D., Orosz, J. A., McClintock, J. E., Remillard, R. A. 1995, *Nature*, 378, 157.
- Beekman, G., Shahbaz, T., Naylor, T., Charles, P. A. 1996, *MNRAS*, 281, L1.
- Brown, G. E., Bethe, H. A. 1994, *ApJ*, 423, 659.
- Brown, G. E., Weingartner, J. C., Wijers, R. A. M. J. 1996, *ApJ*, 463, 297.
- Callanan, P. J. et al. 1996, *ApJ*, 461, 351.
- Casares, J., Charles, P. A., Naylor, T. 1992, *Nature*, 355, 614.
- Casares, J., Charles P. A. 1994, *MNRAS*, 271, L5.
- Casares, J., Martin, E. L., Charles, P. A., Molaro, P., Rebolo, R. 1997, *New Astronomy*, in press.
- Filippenko, A. V., Matheson, T., Ho, L. C. 1995a, *ApJ*, 455, 614.

- Filippenko, A. V., Matheson, T., Barth, A. J. 1995b, ApJ, 455, L139.
- Filippenko, A. V., Matheson, T., Leonard, D. C., Barth, A. J., Van Dyk, S. D. 1997, PASP, 109, 461.
- Finn, L. S. 1994, Phys. Rev. Lett., 75, 1878
- Harlaftis, E. T., Horne, K., Filippenko, A. V. 1996, PASP, 108, 762.
- Harlaftis, E. T., Steeghs, D., Horne, K., Filippenko, A. V. 1997, AJin press.
- Haswell, C. A., Robinson, E. L., Horne, K., Stiening, R. F., Abbott, T. M. C. 1993 ApJ, 411, 802.
- Kolb, U., King, A. R., Ritter, H., Frank, J. 1997, ApJin press.
- Loredo, T. J. 1990 in “Maximum Entropy and Bayesian Methods” ed. P. Fourge‘re, Kluwer: Dordrecht, p. 81.
- Maeder, A. 1992, *â*, 264, 105.
- McClintock, J. E., & Remillard, R. A. 1986, ApJ, 308, 110.
- McClintock, J. E., & Remillard, R. A. 1990, ApJ, 350, 386.
- Orosz, J. A., Bailyn, C. D, Remillard, R. A., McClintock, J. E., & Foltz, C. B. 1994a, ApJ, 436, 848.
- Orosz, J. A., Bailyn, C. D. 1995, ApJ, 446, L59.
- Orosz, J. A., Bailyn, C. D. Remillard, R. A., McClintock, J. E. 1996, ApJ, 468, 380.
- Orosz, J. A., Bailyn, C. D 1997, ApJ, 477, 876.
- Pavlenko, E. P., Martin, A. C., Casares, J., Charles, P. A., Ketsaris, N. A. 1996, MNRAS, 281, 1094.
- Remillard, R. A., McClintock, J. E., & Bailyn, C. D. 1992, ApJ, 399, L145.
- Remillard, R. A., Orosz, J. A., McClintock, J. E., & Bailyn, C. D. 1996, ApJ, 459, 226.
- Shahbaz, T., Naylor, T., Charles, P. A. 1994a, MNRAS, 268, 756.
- Shahbaz, T., Ringwald, F. A., Bunn, J. C., Naylor, T., Charles, P. A., Casares, J. 1994b, MNRAS, 271, L10.

Timmes, F. X., Woosley, S. E., Weaver, T. A. 1995, ApJS, 98, 617.

Timmes, F. X., Woosley, S. E., Weaver, T. A. 1996, ApJ, 457, 834.

Woosley, S. E., Langer, N., Weaver, T. A. 1995, ApJ, 448, 315.

Woosley, S. E., Weaver, T. A. 1995, ApJS101, 181.

Table 1. Observed Constraints on Black Hole Mass

Object	f(m)	q	i
2023+34	6.07 ± 0.05	0.060 ± 0.005	$52 \leq i \leq 60$
2000+25	5.01 ± 0.12	0.042 ± 0.012	$43 \leq i \leq 74$
1705-25	4.65 ± 0.21	0.018 ± 0.016	$60 \leq i \leq 80$
1655-40	3.24 ± 0.09	0.333 ± 0.010	$67 \leq i \leq 71$
1124-68	3.01 ± 0.15	0.13 ± 0.04	$54 \leq i \leq 65$
0620-00	2.91 ± 0.08	0.067 ± 0.010	$31 \leq i \leq 70.5$
0422+32	1.21 ± 0.06	0.049 ± 0.020	$28 \leq i \leq 45$

Table 2. Results of Bayesian Analysis

Sources	max likely m_u	max likely m_l	range m_u	range m_l	relative likelihood
All	11.8	5.0	10.5 ~ 18.0	0.5 ~ 6.9	1
No 0422	11.9	5.0	10.5 ~ 19.4	0.5 ~ 6.9	2.0
No 0620	11.9	5.1	10.5 ~ 18.5	0.5 ~ 6.9	5.6
No 1124	12.1	5.0	10.6 ~ 19.2	0.5 ~ 7.1	5.3
No 1655	12.2	4.8	10.5 ~ 19.5	0.5 ~ 6.8	4.2
No 1705	12.1	5.2	10.5 ~ 19.0	0.5 ~ 7.2	8.8
No 2000	11.9	4.8	10.5 ~ 18.6	0.5 ~ 6.9	6.3
No 2023	6.9	6.8	6.3 ~ 11.0	2.6 ~ 7.5	134.0

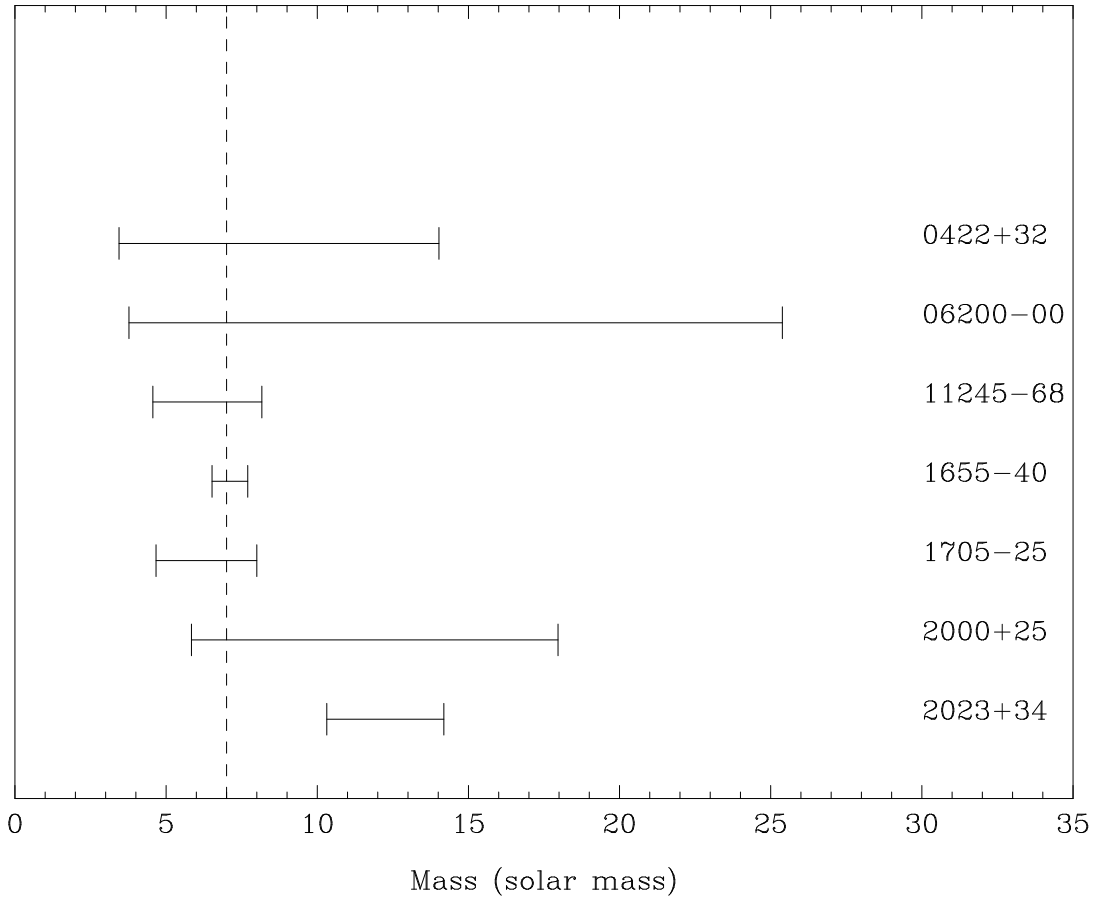


Fig. 1.— Mass ranges for the compact primaries of the seven sources in our sample. Note that it is incorrect to think of these ranges as representing some number of “sigma” about a mean value, due to the strongly non-gaussian nature of the probability distribution.

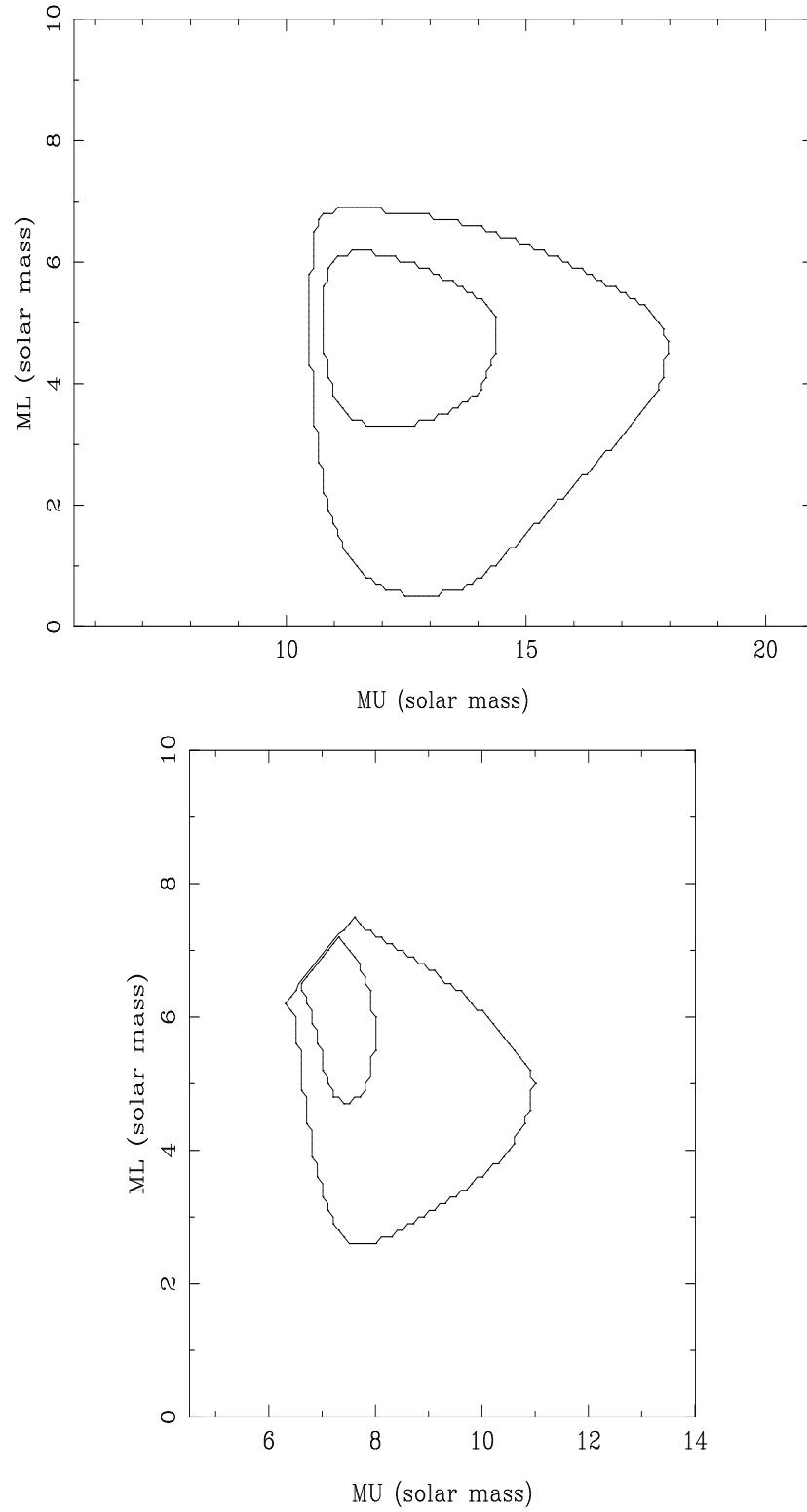


Fig. 2.— Probability contours in the (m_L, m_U) plane. Inner contour contains 50% of the probability; outer contour contains 95% of the probability. Top panel includes GS 2023+34; bottom panel does not.

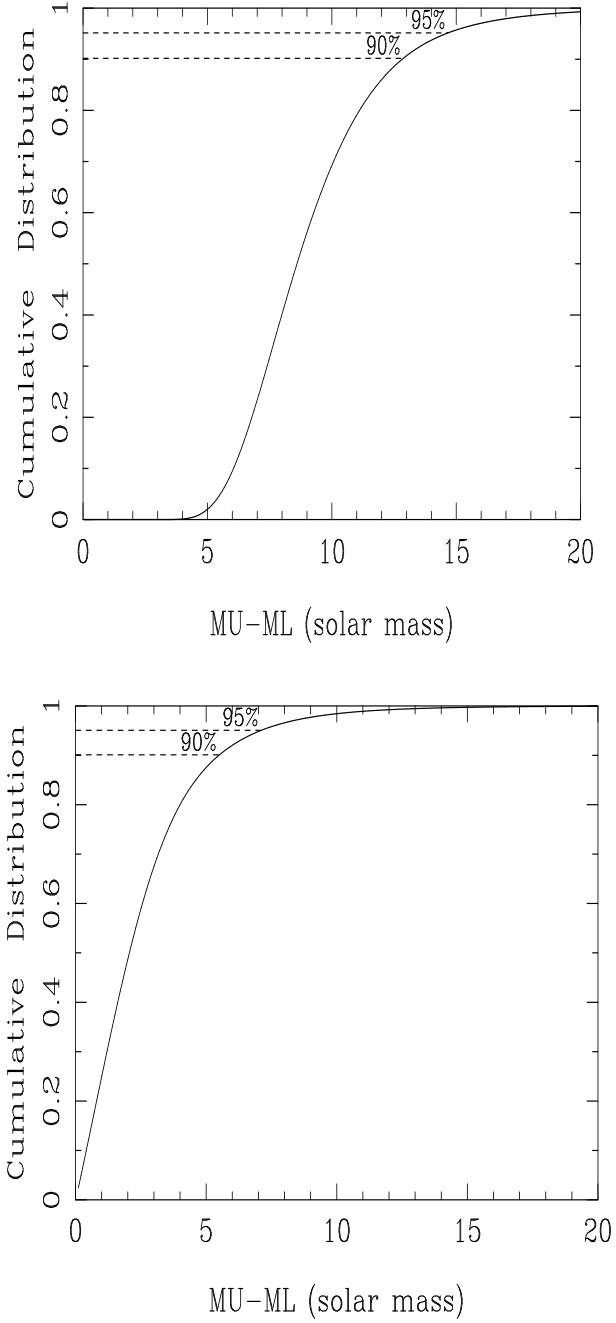


Fig. 3.— Cumulative probability that $m_U - m_L$ is less than a given value. Top panel includes GS 2023+34; bottom panel does not. Note that in the absence of GS 2023+34, a much narrower range of masses is required.

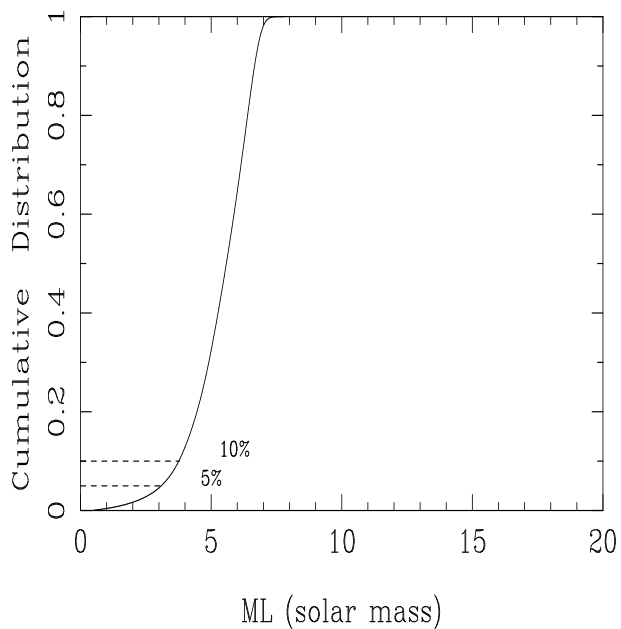
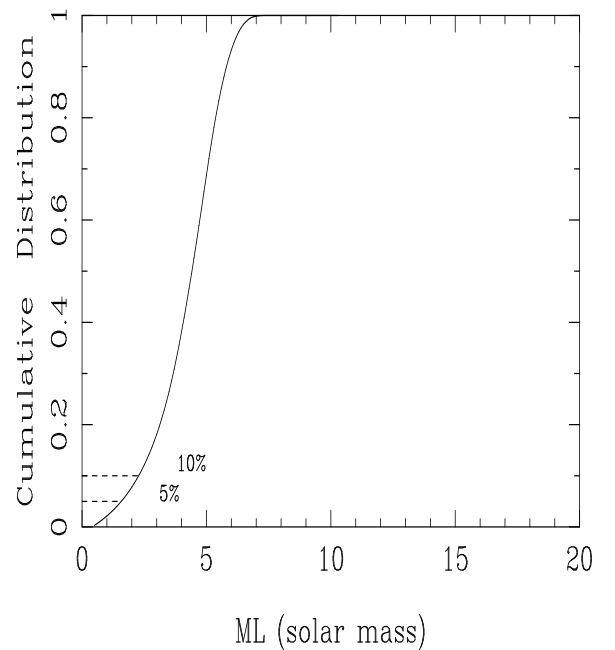


Fig. 4.— Cumulative probability that m_L is below a given value. Top panel includes GS 2023+34; bottom panel does not. Note that in the absence of GS 2023+34, there is a $> 95\%$ probability that $m_L > 3M_\odot$.